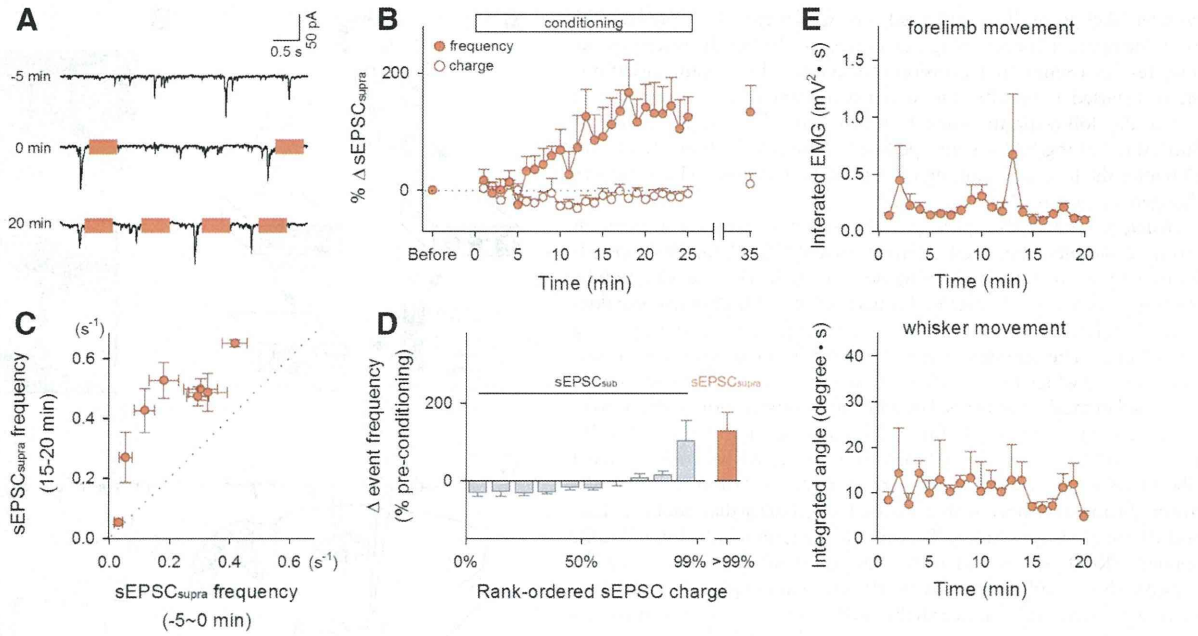

Figure 2. Neurofeedback-mediated reinforcement of sEPSC$_{supra}$s in hippocampal neurons. ***A***, sEPSC traces recorded from a representative neuron at −5, 0, and 20 min relative to the onset of conditioning. Colored bars indicate LH stimulation periods. ***B***, Time courses of the percent changes in the mean frequency (closed circles) and the mean charge (open circles) of sEPSC$_{supra}$s during the 25 min of conditioning. Error bars indicate the SEMs of 9 neurons from 9 mice; 6 of 9 neurons exhibited a significant change in the sEPSC$_{supra}$ frequency. ***C***, The sEPSC$_{supra}$ frequency 15–20 min after the onset of LH stimulation was plotted against that measured 0–5 min before the reinforcement. Each data point represents the mean ± SEM of a single neuron. ***D***, Percent changes in the frequency distribution of sEPSC charges during the postconditioning session relative to the preconditioning baseline. The sEPSC charges were rank ordered and normalized in each experiment. ***E***, During operant conditioning, EMGs were recorded from forelimbs (top) and whisker movement was monitored (bottom). Neither the EMG power nor the whisker movement integral changed in the course of the development of sEPSC$_{supra}$ reinforcement. Error bars indicate the SEMs of three mice.

randomly generated at a mean frequency of 0.1 Hz, which was determined based on the mean stimulation frequency during the reinforcement experiments shown in Figure 2. The randomly timed rewarding electrical stimulation did not induce an increase in sEPSC$_{supra}$ frequency ($p = 0.48$, $t_4 = 0.78$, paired t test, $n = 5$ cells; Fig. 3*B*,*C*, left).

To examine whether sEPSC$_{supra}$ reinforcement is driven by reward stimulation or by contingency of electrical stimulation of the brain, we applied contingent electrical stimulation to the ventromedial thalamus, a reward-unrelated thalamic nucleus that is located close to the LH and projects to the hippocampus (Su and Bentivoglio, 1990; Varela et al., 2013). Stimulation to the ventromedial thalamus was not shown to increase the sEPSC$_{supra}$ frequency, at least during our 25 min observation period ($p = 0.11$, $t_4 = 2.04$, paired t test, $n = 5$ cells; Fig. 3*B*,*C*, left). Therefore, the increased sEPSC$_{supra}$s represent a contingent reward-driven, NMDA-receptor-dependent reinforcement of synaptic activity.

In layer II/III pyramidal cells of the primary somatosensory cortex, which is located immediately above the dorsal hippocampus, LH stimulation did not reinforce the sEPSC$_{supra}$ frequency during our observation period ($p = 0.65$, $t_4 = 0.49$, paired t test, $n = 5$ cells; Fig. 3*F*,*G*). Therefore, hippocampal neurons appeared to be more plastic than somatosensory cortical neurons.

Next, hippocampal CA1 pyramidal neurons were voltage clamped at 0 mV, the reversal potential of glutamatergic receptor-mediated currents, to monitor sIPSCs (Fig. 4). We applied a similar conditioning protocol to sIPSCs; the LH was stimulated with an IPSC larger than the top 1% of the prior distribution of sIPSC charges (sIPSC$_{supra}$) in the patched CA1 neurons (Fig. 4*A*). The mean frequency of sIPSC$_{supra}$ before the conditioning was 0.14 ± 0.02 Hz (mean ± SEM of 5 cells from 5 mice). In the LH reinforcement and yoked control groups, neither the frequencies of sIPSC$_{supra}$s nor those of sIPSC$_{sub}$s changed (sIPSC$_{supra}$: $p = 0.87$, $t_4 = 0.18$, paired t test, $n = 5$ cells for the reinforcement group; $p = 0.79$, $t_2 = 0.31$, $n = 3$ cells for the yoked control; sIPSC$_{sub}$: $p = 0.12$, $t_4 = 1.99$, paired t test for the reinforcement group; $p = 0.40$, $t_2 = 1.05$ for the yoked control; Fig. 4*B*,*C*).

Reinforcement of spiking activity

We sought to link the plasticity of sEPSC$_{supra}$s to a change in spike output. We patch clamped CA1 neurons in the cell-attached configuration and monitored spontaneous spike series. The neurons exhibited two types of spiking patterns, single spikes and transient HFBs of spikes (Kandel and Spencer, 1961; Ranck, 1973). We defined an HFB as an event in which at least three spikes occurred at >100 Hz. The neurons that emitted HFBs at >0.033 Hz (twice per minute) during the preconditioning session were selected, so that mice were sufficiently given reward stimuli while the patch-clamp configuration was maintained. Based on this criterion, approximately 80% of the recorded cells were discarded. In the remaining datasets, HFBs occurred at a mean frequency of 0.12 ± 0.02 Hz (mean ± SEM of 39 cells from 39 mice; see Fig. 9*B*). We then delivered LH stimulation upon HFB occurrence (Fig. 5*A*). HFBs were reinforced in a time course similar to the sEPSC$_{supra}$ conditioning ($p = 8.2 \times 10^{-7}$, $t_{29} = 6.24$, paired t test vs the preconditioning baseline, $n = 30$ cells; Fig. 5*B*,*F*), whereas the frequency of single spikes was not changed ($p = 0.30$, $t_{29} = 1.07$; Fig. 5*G*,*H*). The reinforcement did not occur in MK801-treated mice ($p = 0.85$, $t_4 = 0.20$, paired t test, $n = 5$ cells; $P = 0.032$, Bonferroni's/Dunn's test vs reinforcement' Fig. 5*C*,*F*), yoked control mice ($p = 0.34$, $t_8 = 1.02$, $n = 9$ cells; $p = 0.0014$, Bonferroni's/Dunn's test vs reinforcement; Fig. 5*C*,*F*), or urethane-anesthetized mice ($p = 0.35$, $t_5 = 1.02$, $n = 6$ cells; Fig. 5*I*,*J*), even though MK801 did not alter the HFB frequency dur-

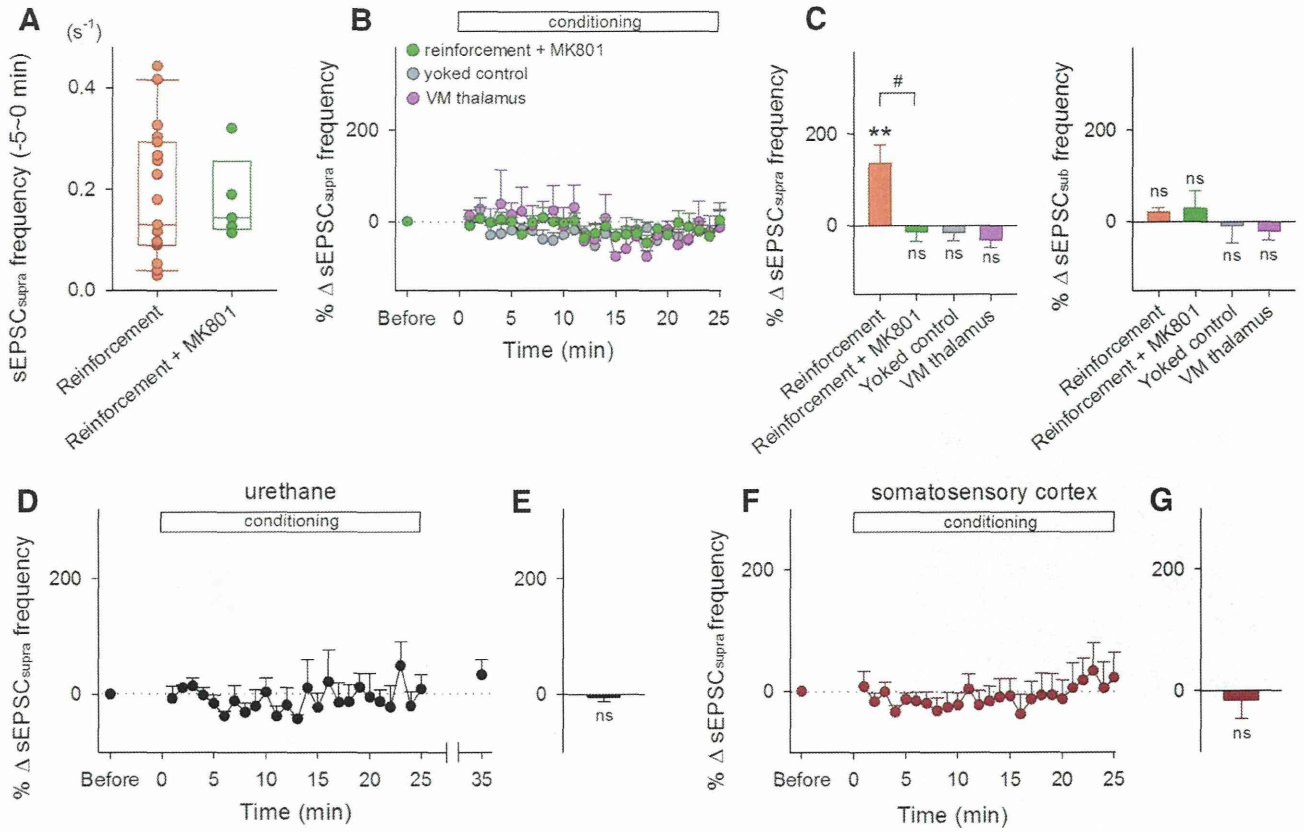

Figure 3. Experimental conditions for $sEPSC_{supra}$ reinforcement. ***A***, Raw data (dots) and the boxplot represent the distribution of baseline frequencies of HFBs in control and MK801-treated mice during the period 0–5 min before the onset of conditioning. The initial frequencies did not differ between two groups. ***B***, Time courses of the percent changes in the $sEPSC_{supra}$ frequency in mice treated with MK801 ($n = 5$), mice with pseudorandom (yoked) conditioning ($n = 5$), and mice that received stimulation of the ventromedial (VM) thalamus ($n = 5$). Error bars indicate SEMs. ***C***, Mean changes in the frequencies of $sEPSC_{supra}$s (left) and $sEPSC_{sub}$s (right) during the period between 15 and 20 min after the onset of conditioning. $^{**}p = 0.0091$ versus preconditioning baseline, paired *t* test; $\#p = 0.021$ versus reinforcement, Bonferroni's/Dunn's test. ***D***, Time courses of the percent changes in the $sEPSC_{supra}$ frequency of during the 25 min of conditioning in urethane-anesthetized mice. Error bars indicate the SEMs of five neurons. ***E***, Mean changes in the $sEPSC_{supra}$ frequency during the 15–20 min period after the onset of conditioning. ***F***, Time courses of the percent changes in the $sEPSC_{supra}$ frequency of layer II/III pyramidal cells in the somatosensory cortex during the 25 min of conditioning. Error bars indicate the SEMs of five neurons. ***G***, Mean changes in the $sEPSC_{supra}$ frequency during the 15–20 min after the onset of conditioning. ns, $p > 0.05$ versus preconditioning baseline of each group, paired *t* test.

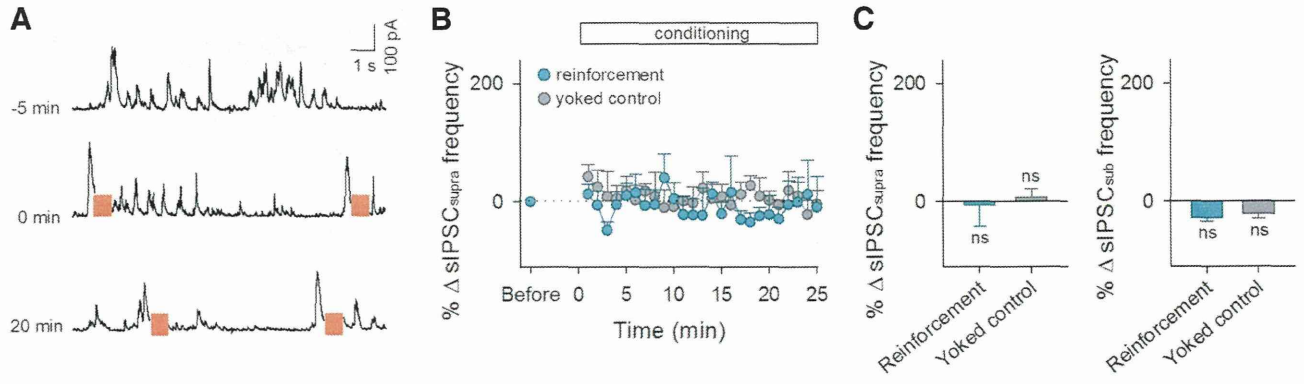

Figure 4. $sIPSC_{supra}$s are not reinforced during the conditioning. ***A***, sIPSC traces recorded from a representative neuron at −5, 0, and 20 min relative to the onset of conditioning. Colored bars indicate LH stimulation periods. ***B***, Time courses of the percent changes in the frequency of $sIPSC_{supra}$s during the conditioning. Error bars indicate the SEMs of five (reinforcement) and three neurons (yoked control). ***C***, Mean changes in the frequencies of $sIPSC_{supra}$s (left) and $sEPSC_{sub}$s (right) during the period between 15 and 20 min after the onset of conditioning. ns, $p > 0.05$ versus preconditioning baseline of each group, paired *t* test.

ing the preconditioning period (0.15 ± 0.03 Hz, mean ± SEM; $p = 0.70$, Bonferroni's/Dunn's test vs reinforcement). To examine the involvement of NMDA receptors in the CA1 region, we injected 300 μM MK801 parenchymally into the CA1 region. The diffusion of MK801 was estimated by SR101 injection (Fig. 5*D*), because MK801 and SR101 are both water-soluble small molecules (MK801: 337 Da; SR101: 601 Da). After the pipette used for local MK801 injection was carefully pulled out from the brain, neurons in MK801-injected areas were patch clamped and the conditioning started within 30 min. Local application of MK801

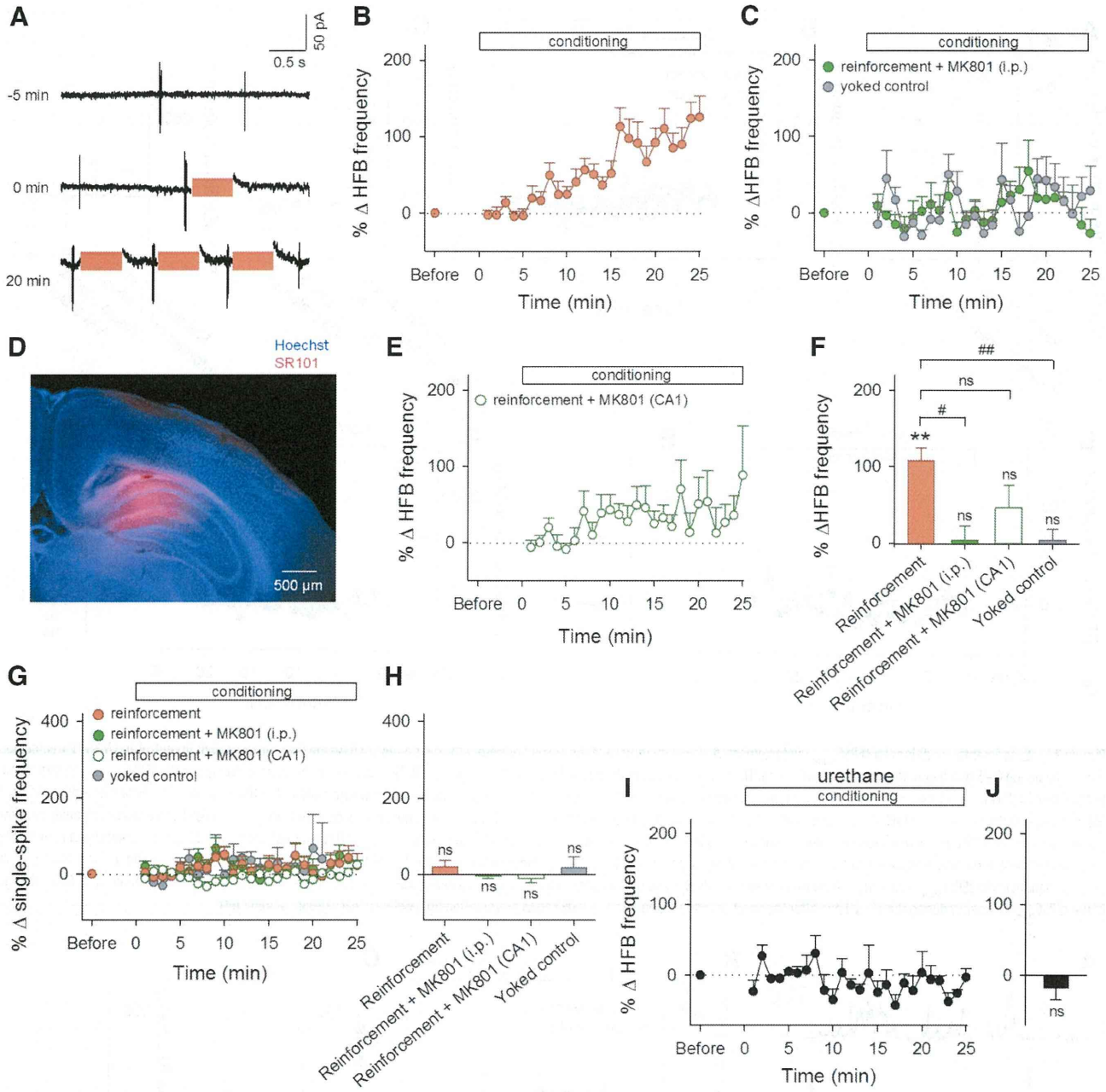

Figure 5. Selective reinforcement of HFBs in unanesthetized and anesthetized mice. ***A***, Unit activity recorded from a representative neuron at −5, 0, and 20 min relative to the onset of conditioning. Colored bars indicate LH stimulation periods. ***B***, Time courses of the percent changes in the frequency of HFB events during the 25 min of conditioning. Error bars indicate the SEMs of 30 neurons (reinforcement). Of 30 neurons, 21 exhibited significant changes in the HFB frequency. ***C***, Time courses of the percent changes in the HFB frequency in mice treated with intraperitoneal MK801 ($n = 5$) and in yoked control mice ($n = 9$). ***D***, Representative image of locally injected SR101 (red) counterstained by Hoechst 33342. ***E***, Time courses of the percent changes in the frequency of HFBs during the 25 min of conditioning in mice injected with MK801 into the CA1 region. ***F***, Mean changes in the HFB frequency during the period between 15 and 20 min after the onset of conditioning. $^{**}p = 8.2 \times 10^{-7}$, ns, $p > 0.05$ versus preconditioning baseline, paired t test; #$p = 0.032$, ##$p = 0.0014$, ns, $p > 0.05$ versus reinforcement, Bonferroni's/Dunn's test. ***G***, Time courses of the percent changes in the frequency of single spikes during the 25 min of conditioning. ***H***, Mean changes in the single-spike frequency during the period between 15 and 20 min after the onset of conditioning. ns, $p > 0.05$ versus preconditioning baseline, paired t test. ***I***, Time courses of the percent changes in the frequency of HFB events during the 25 min of conditioning in urethane-anesthetized mice. Error bars indicate the SEMs of six neurons. ***J***, Mean changes in the HFB frequency during the period between 15 and 20 min after the onset of conditioning. ns, $p > 0.05$ versus preconditioning baseline, paired t test.

attenuated the HFB reinforcement; MK801-treated neurons did not exhibit a significant increase in HFB frequency ($p = 0.16$, $t_7 = 1.59$, paired t test vs baselines, $n = 8$ cells; $p = 0.18$, Bonferroni's/Dunn's test vs reinforcement; Fig. 5*E*,*F*), whereas local application of MK801 did not alter the HFB frequency during the preconditioning period (0.12 ± 0.04 Hz, mean ± SEM; $p = 0.99$, Bonferroni's/Dunn's test vs reinforcement).

To examine the circuit specificity of HFB reinforcement, we conducted cell-attached recordings simultaneously from two CA1 neurons that were located ~200 μm apart from one another. The LH was stimulated upon HFBs in one neuron but not in the other neuron. The conditioned neuron was randomly assigned in each pair. The HFB frequency increased in the conditioned neurons ($p = 0.042$, $t_4 = 2.95$, paired t test, $n = 5$ cells; Fig.

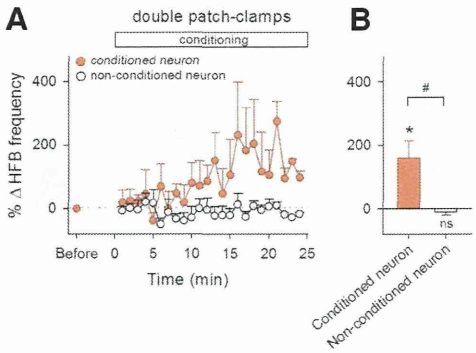

Figure 6. Selective reinforcement of HFBs in a pathway-specific manner. ***A***, Time courses of the HFB frequencies of two simultaneously recorded neurons during the conditioning of one neuron ($n = 5$ pairs). Error bars indicate the SEMs of five pairs. ***B***, Mean changes in the HFB frequencies during the period between 15 and 20 min after the onset of conditioning. $*p = 0.042$; ns, $p > 0.05$ versus preconditioning baseline of each group, paired t test; $\#p = 0.015$, Student's t test.

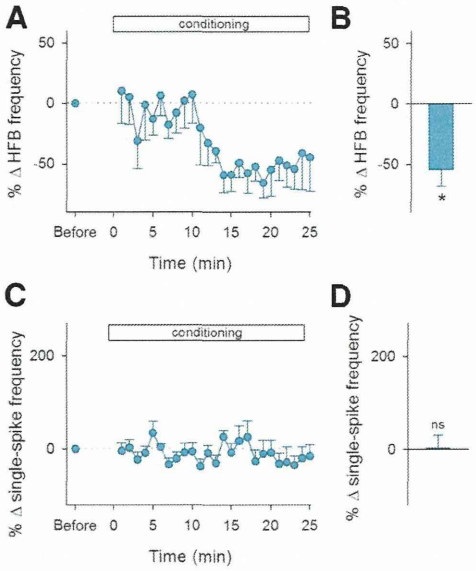

Figure 7. Reinforcement for the disappearance of HFBs. ***A***, Time courses of the HFB frequency during the reinforcement for the disappearance of HFBs. Error bars indicate the SEMs of six neurons. ***B***, Mean changes in the HFB frequency during the period between 15 and 20 min after the onset of conditioning. $*p = 0.011$ versus preconditioning baseline, paired t test. ***C***, Time courses of the percent changes in the frequency of single spikes during the 25 min of conditioning. ***D***, Mean changes in the single-spike frequency during the period between 15 and 20 min after the onset of conditioning. ns, $p > 0.05$ versus preconditioning baseline, paired t test.

6), but not in the nonconditioned ones ($p = 0.37$, $t_4 = 1.02$, paired t test, $n = 5$ cells; $p = 0.015$ for conditioned vs nonconditioned, $t_8 = 3.09$, Student's t test), suggesting pathway specificity of the operant conditioning.

We also tested explicitly nonpaired controls; LH stimulation was applied when HFBs did not occur for a given period. The "endurance" period was set at 6.3 ± 1.2 s such that the initial frequency of LH stimulation was ~0.1 Hz (Fig. 9*B*). With the nonpaired reinforcement, HFBs decreased within 15 min ($p = 0.011$, $t_5 = 3.92$, paired t test, $n = 6$ cells; Fig. 7*A*,*B*) without a change in the frequency of single spikes ($p = 0.96$, $t_5 = 0.05$; Fig. 7*C*,*D*).

Ripple reinforcement

To relate the HFB reinforcement to hippocampal network activity, we recorded LFPs from the CA1 stratum pyramidale and compared the timings of HFBs and ripple events, transient high-frequency oscillations in the hippocampus (Buzsáki et al., 1992) (Fig. 8*A*). During the preconditioning period, the event frequency of ripples was 0.20 ± 0.03 Hz (mean ± SEM of 5 mice) and was significantly higher than that of HFBs ($p = 0.024$, $t_4 = 3.55$, paired t test, $n = 5$ mice). The coincidence ratio of HFBs and ripples was as low as 0.017 ± 0.003 (mean ± SEM of 5 mice). Nonetheless, HFBs and ripples were both reinforced when HFBs were conditioned regardless of ripple occurrence ($p = 0.0017$, $t_4 = 7.51$, paired t test, $n = 5$ cells from 5 mice for HFBs; $p = 0.0018$, $t_4 = 7.41$, paired t test, $n = 5$ mice for ripples; Fig. 8*B*,*C*). This concomitant reinforcement was not dependent on the initial coincidence ratios of HFBs and ripples (Fig. 8*D*). In 4 of 5 mice, the conditioning increased the coincidence ratios (Fig. 8*E*). We also found that ripple events per se could be reinforced: when ripple event timings were targeted for reward stimulation, the frequency of ripples started to increase ~5–10 min after the onset of the conditioning and reached an increased level of 151.7 ± 54.3% after 20–25 min ($p = 0.038$, $t_5 = 2.79$, paired t test, $n = 6$ mice; Fig. 8*F*).

Effect of motivation on HFB reinforcement

The operant conditioning of HFBs did not occur in mice that received intraperitoneal administration of 50 μg/kg SCH23390, a selective dopamine D_1 receptor antagonist, 15–30 min before the conditioning ($p = 0.71$, $t_9 = 0.50$, paired t test, $n = 10$ cells; Fig. 9*A*), whereas SCH23390 did not alter the baseline frequency of HFBs before the conditioning ($p = 0.18$, Bonferroni's/Dunn's test vs reinforcement; Fig. 9*B*). Dopamine is believed to be associated with reward and internal motivation (Salamone and Correa, 2012). Therefore, to examine whether mice under conditions of depression and anxiety can acquire HFB conditioning, we conducted a forced swimming test, a behavioral despair model (Porsolt et al., 1977), to burden mice with acute stress. This acute stress is known to cause various aberrations of the morphology and electrophysiological properties of hippocampal neurons (Howland and Wang, 2008; Maras and Baram, 2012). Mice were placed in a water-filled cylinder for 15 min until they spent approximately 60% of their time in immobility (Fig. 9*C*, day 1). In these acutely stressed mice, the baseline frequency of HFBs was not different from that of control mice ($p = 0.23$, Bonferroni's/Dunn's test vs reinforcement; Fig. 9*B*), but LH stimulation did not reinforce the HFB frequency ($p = 0.40$, $t_9 = 0.89$, paired t test, $n = 10$ cells; Fig. 9*D*,*F*).

As another series of experiments, the stressed mice were again placed in the same water-filled cylinder for 5 min on the next day. They spent 51.8 ± 3.6% of their time in immobility (mean ± SEM of 10 vehicle-treated mice; Fig. 9*C*). This immobility period was reduced to 29.5 ± 3.0% in stressed mice that had been repeatedly administered with 20 mg/kg fluoxetine between the day 1 and day 2 tests (mean ± SEM of 8 fluoxetine-treated mice; $p = 0.0003$, $t_{16} = 4.62$, Student's t test; Fig. 9*C*). After the day 2 test, the stressed mice failed to exhibit HFB reinforcement ($p = 0.61$, $t_9 = 0.52$, paired t test, $n = 10$ cells; Fig. 9*E*,*F*); however, this depressive effect was rescued in fluoxetine-treated mice ($p = 0.028$, $t_7 = 2.77$, paired t test, $n = 8$ cells, $p = 0.021$, $t_{16} = 2.78$, Student's t test; Fig. 9*E*,*F*). Neither day 2 forced swimming stress nor fluoxetine treatment changed the baseline HFB frequency during the preconditioning period ($p = 0.67$, Bonferroni's/Dunn's test for day 2 forced swimming stress group vs reinforce-

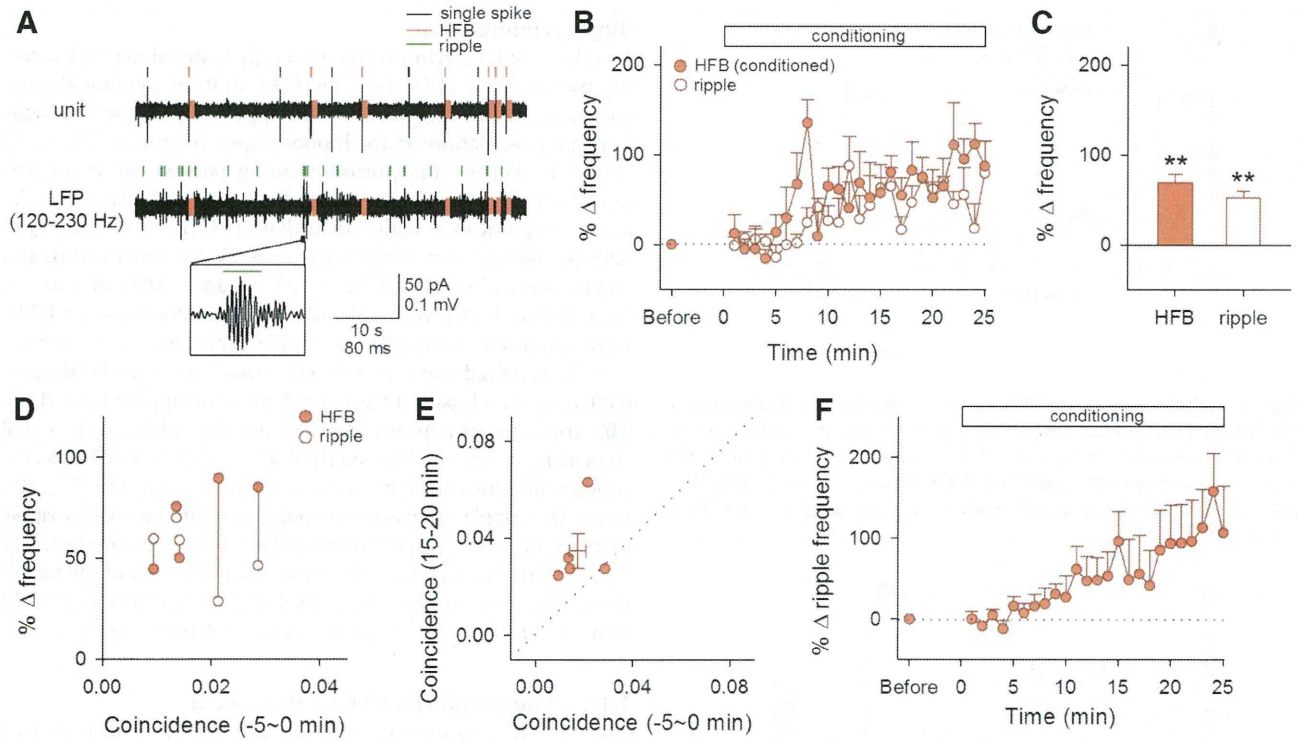

Figure 8. Effect of HFB conditioning on ripples. ***A***, Representative traces of cell-attached unit recording and LFP recording. A ripple event is magnified in the inset. ***B***, Time courses of the percent changes in the frequency of HFBs and ripples during the 25 min of conditioning to HFBs. Error bars indicate the SEMs of five neurons from five mice. ***C***, Mean changes in the frequency of HFBs and ripples 15–20 min after the onset of conditioning. $^{**}p < 0.005$ versus preconditioning baseline of each group, paired *t* test. ***D***, The mean changes in the frequency of HFBs (closed circles) and ripples (open circles) 15–20 min after the conditioning were plotted against the coincidence ratios of HFBs and ripples 0–5 min before the reinforcement. Each data point represents the mean of a single neuron. Simultaneously recorded data are linked with vertical lines. ***E***, The coincidence ratios 0–5 min before and 15–20 min after the reinforcement was plotted. Each symbol represents the mean of a single neuron and their means ± SEM are shown by lines. ***F***, Time courses of the percent changes in the frequency of ripples during the 25 min of conditioning to ripples. Error bars are SEMs of six mice.

ment; $p = 1.00$, Bonferroni's/Dunn's test for fluoxetine-treated group vs reinforcement; Fig. 9*B*).

Discussion

In this study, we demonstrated that some form of hippocampal neuronal activity could be rapidly and selectively reinforced by contingent rewards through a neurofeedback operant conditioning paradigm without any pretraining session. The findings include the following: (1) this reinforcement learning emerged as an NMDA receptor-dependent internal neural process without apparent body movement; (2) the reinforcement did not occur under anesthesia, in marked contrast to involuntary learning that can occur under anesthesia, such as fear conditioning (Weinberger et al., 1984; Rosenkranz and Grace, 2002); and (3) LH stimulation did not work as a motivational reward in mice under stressed or depressed conditions.

Previous studies on operant conditioning of single-cell activity have emphasized the firing rates of neocortical neurons in the motor cortex (Fetz, 1969; Fetz and Finocchio, 1975), prefrontal (Kobayashi et al., 2010; Schafer and Moore, 2011), and temporal cortex (Cerf et al., 2010) rather than hippocampal neurons in primates including humans. The subjects had to be trained or pretested in neural decoding for hours or days, combined with external reward and motor/perceptual modulation, before they could control cortical unit activity (Fetz, 2007). Therefore, our experimental approach was unique in the following ways: (1) naive, untrained mice were used, (2) the internal reward was applied electrophysiologically, (3) neurons of the hippocampus were conditioned, and (4) subthreshold synaptic activity was monitored. Under these novel conditions, we succeeded in reinforcing sEPSCs within 15 min. Because mice are useful in molecular biology and genetics studies, our work will help bridge the gap between a behavioral operant and the underlying molecular mechanisms.

Spike rates of pyramidal cells in CA1 are reported to conform to a lognormal distribution with the median HFB event rate being approximately 0.01 Hz (Mizuseki and Buzsáki, 2013). The firing rates of hippocampal neurons recorded in our experiments were higher than those reported previously. This difference is mainly because we did not use ~80% neurons, which emitted HFBs at <0.033 Hz. It is also possible that cell-attached recordings per se affected the excitability of the recorded neurons (Alcami et al., 2012). Whether neurons with lower firing rates can also be reinforced remains to be addressed.

The reinforcement required NMDA receptor activity. NMDA receptors are known to be involved in the induction of synaptic plasticity in hippocampal excitatory transmission. Indeed, the HFB conditioning efficiency was reduced by local injection of an NMDA receptor antagonist into the CA1 region. Therefore, a simple explanation for the neural operant is that CA3-to-CA1 synapses in the recorded CA1 neurons exhibited long-term potentiation during the reinforcement. However, we do not believe that this scenario can completely account for our results, because local MK801 injection only partially prevented the HFB reinforcement. Moreover, the $sEPSC_{supra}$ reinforcement increased

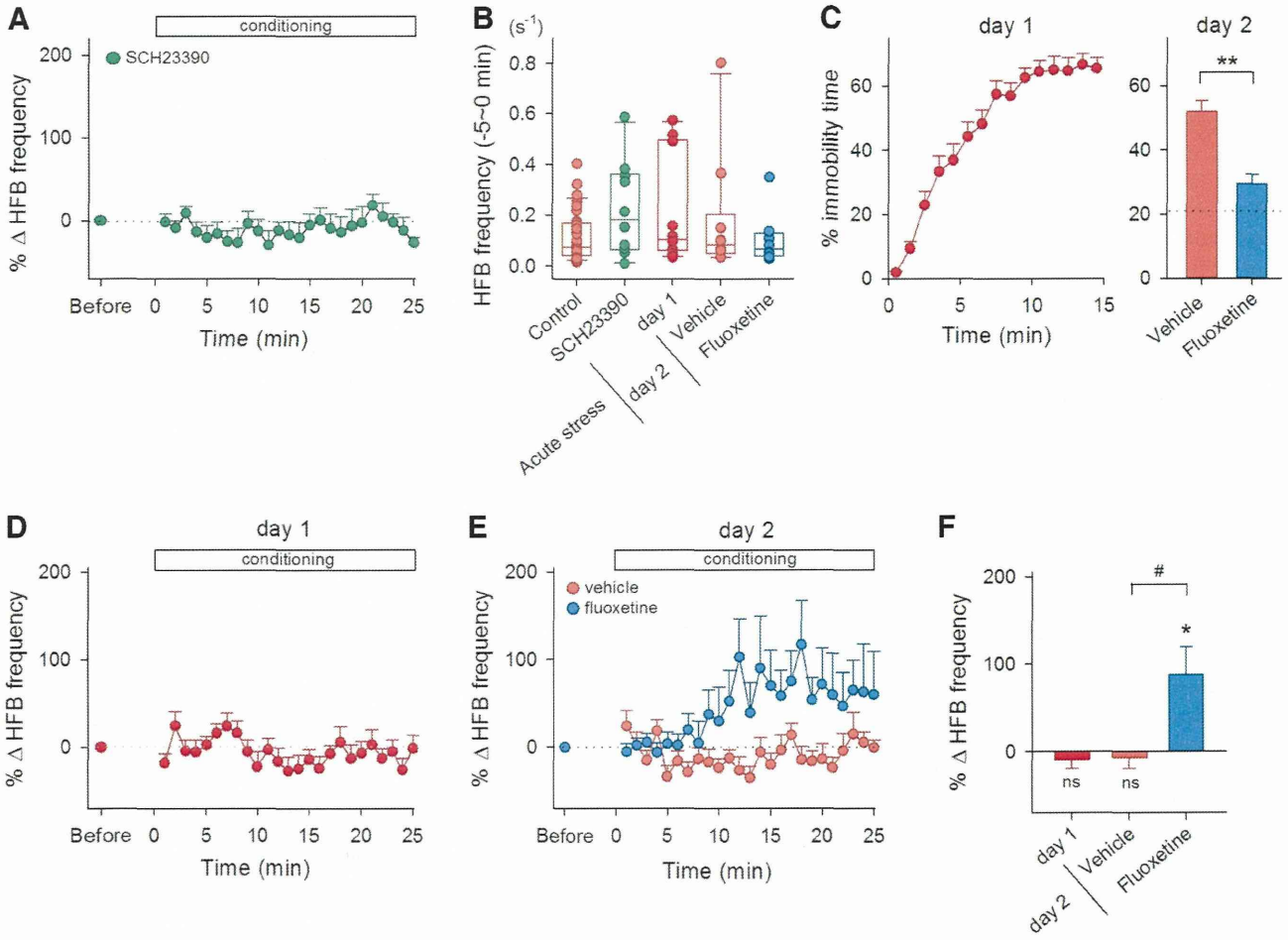

Figure 9. A lack of HFB reinforcement in stressed or depression-model mice. ***A***, Time courses of the percent changes in the HFB frequency during the conditioning in SCH23390-treated mice ($n = 10$). ***B***, Raw data (dots) and the boxplot represent the distribution of baseline frequencies of HFBs in control, SCH23390-treated, and acutely stressed mice during the period 0–5 min before the onset of conditioning. There were no statistical differences in the initial frequency across the groups versus reinforcement, Bonferroni's/Dunn's test. ***C***, The percentage of time spent for immobility during every 1 min period (day 1) or during the total 5 min (day 2) in a water-filled cylinder in vehicle-treated and fluoxetine-treated mice. The horizontal line in the right panel indicates the mean value of the first 5 min in naive mice in the day 1 test. Fluoxetine was administered 3 times between the day 1 and day 2 tests. $^{**}p = 0.0003$ versus vehicle group, Student's *t* test. ***D***, Time courses of the percent changes in the HFB frequency during the conditioning in acutely stressed mice that experienced the day 1 test ($n = 10$). ***E***, Time courses of the HFB frequency in mice treated with saline ($n = 10$) or fluoxetine ($n = 8$) after the day 2 test. ***F***, Mean changes in the HFB frequency during the period between 15 and 20 min after the onset of conditioning in acutely stressed mice (day 1) and in stressed mice treated with vehicle or fluoxetine (day 2). $\#p = 0.021$ versus vehicle group, Student's *t* test; $^{*}p = 0.028$; ns, $p > 0.05$ versus preconditioning baseline of each group, paired *t* test.

their frequencies, but not their charges. This result suggests that the conditioned CA1 pyramidal neuron came to receive synaptic inputs more frequently from specific assemblies of CA3 presynaptic neurons, rather than to receive stronger synaptic inputs from these CA3 neurons or to recruit more numbers of CA3 neurons. This notion seems consistent with two observations: first, the $sEPSC_{supra}$ or HFB conditioning did not alter the frequency of $sEPSC_{sub}$s or single spikes and, second, the HFB conditioning of one neuron did not alter the HFB frequency of the unconditioned neuron in a simultaneously recorded neuron pair. We consider the involvement of NMDA receptors to be outside of the CA1 region (perhaps CA3), because the preventing effect of systemic MK801 on the HFB conditioning was stronger than that of local MK801. The reinforcement may emerge from CA3 network reorganization through NMDA-receptor-dependent synaptic plasticity so that specific activities of CA3 ensembles are more frequently sent to the targeted CA1 neurons. Another possible involvement of NMDA receptors is the modulation of dopaminergic neurons of the ventral tegmental area. Phasic firings of these neurons are impaired in mice lacking the NR1 subunit of NMDA receptors in the dopaminergic neurons (Zweifel et al., 2009), which projects to the hippocampus (Oades and Halliday, 1987). Therefore, NMDA receptor blockade may decrease the efficiency of the LH stimulation by altering the firing properties of ventral tegmental area neurons. To confirm this idea, local injection with SCH23390 is required because dopamine D_1 receptors are widely expressed in both reward-related and reward-unrelated brain regions, including the ventral tegmental area, the medial prefrontal cortex, and the hippocampus.

Barrage activities of hippocampal CA1 neurons, such as $sEPSC_{supra}$s and HFBs, originate in the CA3 network and are most likely to be associated with ripple (or sharp-wave) events in LFPs (Ylinen et al., 1995; Maier et al., 2011). One of the simplest mechanisms for the reinforcement of $sEPSC_{supra}$s and HFBs is that animals learned merely to increase the ripple event frequency. However, this mechanism is unlikely. Although we found that the HFB reinforcement was accompanied by an increase of ripple events, the mean frequency of HFBs was lower than that of ripple events, which is consistent with previous reports showing that CA1 pyramidal cells sparsely discharge burst

spikes during ripple oscillations (Ylinen et al., 1995; Csicsvari et al., 1999). Moreover, the coincidence ratio between HFBs and ripples was always <0.1. Interestingly, this ratio increased after the HFB conditioning. Therefore, there is no doubt that the conditioning of single neuron activity induced a change in local network activity. Conversely, our dual cell-attached recordings ($n = 5$) revealed that conditioning of one neuron did not affect the activity of the other neurons. In the recordings, HFBs were rarely coincident between two neurons. Therefore, these neurons were unlikely to be involved in the identical cell assemblies that constitute ripples. This may be a reason why the activities of two neurons could be modulated independently. Consistent with this idea, King et al. (1999) has reported that, when depolarizing currents are injected into a CA1 pyramidal cell simultaneously with spontaneous ripples, its synapses are selectively potentiated.

Inhibitory interneurons are also known to shape ripples/sharp waves (Klausberger et al., 2003), but we failed to reinforce $sIPSC_{supra}$s during our experimental periods. This may be because inhibitory interneurons are less plastic than pyramidal cells and require additional time for reinforcement or because they are connected with pyramidal cells in a less selective manner (Kerlin et al., 2010; Fino and Yuste, 2011; Packer and Yuste, 2011) and cannot be reinforced by operant conditioning of a specific neural pathway. However, we do not rule out the involvement of inhibitory interneurons in the reinforcement. For example, CA3 axo-axonic cells are reported to reduce their firing rates by septum-driven inhibition during ripples and may trigger ripple events (Viney et al., 2013). It is possible that the modulation of their activity patterns contributes to the conditioning of CA1 neuronal activity.

References

Alcami P, Franconville R, Llano I, Marty A (2012) Measuring the firing rate of high-resistance neurons with cell-attached recording. J Neurosci 32:3118–3130. CrossRef Medline

Basmajian JV (1963) Control and training of individual motor units. Science 141:440–441. CrossRef Medline

Buzsáki G (2010) Neural syntax: cell assemblies, synapsembles, and readers. Neuron 68:362–385. CrossRef Medline

Buzsáki G, Leung LW, Vanderwolf CH (1983) Cellular bases of hippocampal EEG in the behaving rat. Brain Res 287:139–171. Medline

Buzsáki G, Horváth Z, Urioste R, Hetke J, Wise K (1992) High-frequency network oscillation in the hippocampus. Science 256:1025–1027. CrossRef Medline

Cerf M, Thiruvengadam N, Mormann F, Kraskov A, Quiroga RQ, Koch C, Fried I (2010) On-line, voluntary control of human temporal lobe neurons. Nature 467:1104–1108. CrossRef Medline

Csicsvari J, Hirase H, Czurkó A, Mamiya A, Buzsáki G (1999) Fast network oscillations in the hippocampal CA1 region of the behaving rat. J Neurosci 19:RC20. Medline

Domjan M, Grau JW (2003) The principles of learning and behavior, Ed 5. Australia, California: Thomson/Wadsworth.

Fetz EE (1969) Operant conditioning of cortical unit activity. Science 163:955–958. CrossRef Medline

Fetz EE (2007) Volitional control of neural activity: implications for brain-computer interfaces. J Physiol 579:571–579. CrossRef Medline

Fetz EE, Finocchio DV (1975) Correlations between activity of motor cortex cells and arm muscles during operantly conditioned response patterns. Exp Brain Res 23:217–240. Medline

Fino E, Yuste R (2011) Dense inhibitory connectivity in neocortex. Neuron 69:1188–1203. CrossRef Medline

Harris KD, Csicsvari J, Hirase H, Dragoi G, Buzsáki G (2003) Organization of cell assemblies in the hippocampus. Nature 424:552–556. CrossRef Medline

Hebb DO (1949) The organization of behavior; a neuropsychological theory. New York: Wiley.

Howland JG, Wang YT (2008) Synaptic plasticity in learning and memory: stress effects in the hippocampus. Prog Brain Res 169:145–158. CrossRef Medline

Kandel ER, Spencer WA (1961) Electrophysiology of hippocampal neurons. II. After-potentials and repetitive firing. J Neurophysiol 24:243–259. Medline

Kerlin AM, Andermann ML, Berezovskii VK, Reid RC (2010) Broadly tuned response properties of diverse inhibitory neuron subtypes in mouse visual cortex. Neuron 67:858–871. CrossRef Medline

King C, Henze DA, Leinekugel X, Buzsáki G (1999) Hebbian modification of a hippocampal population pattern in the rat. J Physiol 521:159–167. CrossRef Medline

Klausberger T, Magill PJ, Márton LF, Roberts JD, Cobden PM, Buzsáki G, Somogyi P (2003) Brain-state- and cell-type-specific firing of hippocampal interneurons in vivo. Nature 421:844–848. CrossRef Medline

Kobayashi S, Schultz W, Sakagami M (2010) Operant conditioning of primate prefrontal neurons. J Neurophysiol 103:1843–1855. CrossRef Medline

Lee AK, Wilson MA (2002) Memory of sequential experience in the hippocampus during slow wave sleep. Neuron 36:1183–1194. CrossRef Medline

Maier N, Tejero-Cantero A, Dorrn AL, Winterer J, Beed PS, Morris G, Kempter R, Poulet JF, Leibold C, Schmitz D (2011) Coherent phasic excitation during hippocampal ripples. Neuron 72:137–152. CrossRef Medline

Maras PM, Baram TZ (2012) Sculpting the hippocampus from within: stress, spines, and CRH. Trends Neurosci 35:315–324. CrossRef Medline

Margules DL, Olds J (1962) Identical "feeding" and "rewarding" systems in the lateral hypothalamus of rats. Science 135:374–375. CrossRef Medline

Mizuseki K, Buzsáki G (2013) Preconfigured, skewed distribution of firing rates in the hippocampus and entorhinal cortex. Cell reports 4:1010–1021. CrossRef Medline

Oades RD, Halliday GM (1987) Ventral tegmental (A10) system: neurobiology. 1. Anatomy and connectivity. Brain Res 434:117–165. Medline

Packer AM, Yuste R (2011) Dense, unspecific connectivity of neocortical parvalbumin-positive interneurons: a canonical microcircuit for inhibition? J Neurosci 31:13260–13271. CrossRef Medline

Porsolt RD, Le Pichon M, Jalfre M (1977) Depression: a new animal model sensitive to antidepressant treatments. Nature 266:730–732. CrossRef Medline

Ranck JB Jr (1973) Studies on single neurons in dorsal hippocampal formation and septum in unrestrained rats. I. Behavioral correlates and firing repertoires. Exp Neurol 41:461–531. Medline

Rosenkranz JA, Grace AA (2002) Dopamine-mediated modulation of odour-evoked amygdala potentials during Pavlovian conditioning. Nature 417:282–287. CrossRef Medline

Sakurai Y, Takahashi S (2013) Conditioned enhancement of firing rates and synchrony of hippocampal neurons and firing rates of motor cortical neurons in rats. Eur J Neurosci 37:623–639. CrossRef Medline

Salamone JD, Correa M (2012) The mysterious motivational functions of mesolimbic dopamine. Neuron 76:470–485. CrossRef Medline

Schafer RJ, Moore T (2011) Selective attention from voluntary control of neurons in prefrontal cortex. Science 332:1568–1571. CrossRef Medline

Su HS, Bentivoglio M (1990) Thalamic midline cell populations projecting to the nucleus accumbens, amygdala, and hippocampus in the rat. J Comp Neurol 297:582–593. CrossRef Medline

Varela C, Kumar S, Yang JY, Wilson MA (2013) Anatomical substrates for direct interactions between hippocampus, medial prefrontal cortex, and the thalamic nucleus reuniens. Brain Struct Funct. Advance online publication. doi:10.1007/s00429-013-0543-5. CrossRef Medline

Viney TJ, Lasztoczi B, Katona L, Crump MG, Tukker JJ, Klausberger T, Somogyi P (2013) Network state-dependent inhibition of identified hippocampal CA3 axo-axonic cells in vivo. Nat Neurosci 16:1802–1811. CrossRef Medline

Weinberger NM, Gold PE, Sternberg DB (1984) Epinephrine enables Pavlovian fear conditioning under anesthesia. Science 223:605–607. CrossRef Medline

Wilson MA, McNaughton BL (1994) Reactivation of hippocampal ensemble memories during sleep. Science 265:676–679. CrossRef Medline

Ylinen A, Bragin A, Nádasdy Z, Jandó G, Szabó I, Sik A, Buzsáki G (1995) Sharp wave-associated high-frequency oscillation (200 Hz) in the intact hippocampus: network and intracellular mechanisms. J Neurosci 15:30–46. Medline

Zweifel LS, Parker JG, Lobb CJ, Rainwater A, Wall VZ, Fadok JP, Darvas M, Kim MJ, Mizumori SJ, Paladini CA, Phillips PE, Palmiter RD (2009) Disruption of NMDAR-dependent burst firing by dopamine neurons provides selective assessment of phasic dopamine-dependent behavior. Proc Natl Acad Sci U S A 106:7281–7288. CrossRef Medline

EJN EUROPEAN JOURNAL OF NEUROSCIENCE FENS

European Journal of Neuroscience, Vol. 39, pp. 2027–2036, 2014 doi:10.1111/ejn.12554

NEUROSYSTEMS

Interneuron firing precedes sequential activation of neuronal ensembles in hippocampal slices

Takuya Sasaki,[1] Norio Matsuki[1] and Yuji Ikegaya[1,2]
[1]Graduate School of Pharmaceutical Sciences, University of Tokyo, Tokyo, Japan
[2]Center for Information and Neural Networks, Suita City, Osaka, Japan

Keywords: circuit, hippocampus, imaging, interneuron, sequence

Abstract

Neuronal firing sequences that occur during behavioral tasks are precisely reactivated in the neocortex and the hippocampus during rest and sleep. These precise firing sequences are likely to reflect latent memory traces, and their reactivation is believed to be essential for memory consolidation and working memory maintenance. However, how the organized repeating patterns emerge through the coordinated interplay of distinct types of neurons remains unclear. In this study, we monitored ongoing spatiotemporal firing patterns using a multi-neuron calcium imaging technique and examined how the activity of individual neurons is associated with repeated ensembles in hippocampal slice cultures. To determine the cell types of the imaged neurons, we applied an optical synapse mapping method that identifies network connectivity among dozens of neurons. We observed that inhibitory interneurons exhibited an increase in their firing rates prior to the onset of repeating sequences, while the overall activity level of excitatory neurons remained unchanged. A specific repeating sequence emerged preferentially after the firing of a specific interneuron that was located close to the neuron first activated in the sequence. The times of repeating sequences could be more precisely predicted based on the activity patterns of inhibitory cells than excitatory cells. In line with these observations, stimulation of a single interneuron could trigger the emergence of repeating sequences. These findings provide a conceptual framework that interneurons serve as a key regulator of initiating sequential spike activity.

Introduction

The reactivation of structured spike patterns in neuronal populations has been assumed to be essential for encoding, consolidation and retrieval of memory in the cortex (O'Neill *et al.*, 2010; Schwindel & McNaughton, 2011). A series of recent studies has demonstrated that the firing sequences that emerge during alert wakefulness are replayed on a millisecond time scale during sharp wave and ripples (SW-Rs) in the hippocampus (Foster & Wilson, 2006; Diba & Buzsaki, 2007; Karlsson & Frank, 2009; Dragoi & Tonegawa, 2011). The repetition of distinct firing modules has also been observed in discharge patterns in the neocortex during transitions from Down to Up states (Luczak *et al.*, 2007), and even in *in vitro* cortical slices (Mao *et al.*, 2001; Ikegaya *et al.*, 2004; MacLean *et al.*, 2005; Matsumoto *et al.*, 2013). Therefore, reactivated patterns are inherent to the cortical network system and could arise from complex interactions between local neuronal ensembles. However, how these specific patterns are created by the dynamic balance between excitatory and inhibitory neuronal activity remains unclear.

In this study, we examined how the timing of repeating sequences is associated with individual spikes by using functional multi-neuron calcium imaging (fMCI), an optical recording technique that monitors neuronal firing based on changes in the somatic fluorescence intensity of a calcium-sensitive indicator (Takahashi *et al.*, 2007; Sasaki *et al.*, 2008). We used a slice culture preparation as our experimental model for the following reasons: (1) it enabled us to record the ongoing activity of hundreds of cells with high spatiotemporal resolution because of low optical scattering (Takahashi *et al.*, 2011); and (2) it preserved the local circuits essential for generating SW-Rs resembling *in vivo* SW-Rs (Maier *et al.*, 2003; Takahashi *et al.*, 2010).

Although the optical imaging technique has revealed multi-neuronal dynamics in various systems (Ikegaya *et al.*, 2004; Ohki *et al.*, 2006; Busche *et al.*, 2008; Bandyopadhyay *et al.*, 2010; Komiyama *et al.*, 2010; Margolis *et al.*, 2012; Ziv *et al.*, 2013), a primary shortcoming of this imaging method is the difficulty in identifying neuronal cell types: excitatory and inhibitory cells cannot be identified by their fluorescence images alone. To circumvent this technical issue, we employed a synapse mapping method termed reverse optical trawling (ROTing), which can identify presynaptic neurons that have monosynaptic connections with patch-clamped neurons (Sasaki *et al.*, 2009; Takahashi *et al.*, 2010). By applying the ROTing method to hippocampal slices, we functionally detected inhibitory neurons in an imaged area and analysed the spatiotemporal activity patterns of excitatory and inhibitory neurons. We discovered that inhibitory neurons increased their firing rates prior to the emergence of repeating sequences, whereas such preceding activity changes were not observed in excitatory pyramidal cells. These results indicate that interneurons provide a temporal fidelity for the sequential activation of ensemble neuronal activity in the cortex.

Correspondence: Dr T. Sasaki, as above.
E-mail: t.sasaki.0224@gmail.com

Received 23 September 2013, revised 5 February 2014, accepted 11 February 2014

Materials and methods

Animal ethics

All experiments were performed with the approval of the animal experiment ethics committee at the University of Tokyo (approval number 19–35), and in accordance with NIH guidelines for the care and use of animals.

Slice preparation

Hippocampal slice cultures were prepared from postnatal day 7 Wistar/ST rats (SLC), as previously described (Koyama *et al.*, 2007). Briefly, rat pups were chilled with ice and decapitated. The brains were removed and cut into 300-μm-thick horizontal slices with a DTK-1500 vibratome (Dosaka, Kyoto, Japan) in aerated, ice-cold Gey's balanced salt solution supplemented with 25 mM glucose. Entorhino-hippocampal stumps were excised and cultured on Omnipore membrane filters (JHWP02500; Millipore, Bedford, MA, USA) that were laid on plastic O-ring disks. The cultures were grown with 1 mL of 50% minimal essential medium, 25% Hank's balanced salt solution and 25% horse serum (Cell Culture Laboratory, Cleveland, OH, USA) in a humidified incubator at 37 °C in 5% CO_2. The medium was changed every 3.5 days.

Recording ongoing activity with fMCI

On days 6–12 *in vitro*, slices were incubated with 2 mL of dye solution at 37 °C for 1 h (Takahashi *et al.*, 2007). The dye solution consisted of artificial cerebrospinal fluid (aCSF) containing 0.0005% Oregon Green 488 BAPTA-1 (OGB-1) AM, 0.01% Pluronic F-127 and 0.005% Cremophor EL. The aCSF was composed of (in mM): NaCl, 127; $NaHCO_3$, 26; KCl, 3.3; KH_2PO_4, 1.24; $MgSO_4$, 1.5; $CaCl_2$, 1.5; glucose, 10. After 30 min of recovery, a slice was transferred to a recording chamber and perfused with aCSF at 28–32 °C at a perfusion rate of 1.5–2.0 mL/min. Fluorophores were excited by the 488-nm line of an argon–krypton laser (5–10 mW, 641-YB-A01; Melles Griot, Carlsbad, CA, USA) and visualized through a 507-nm long-pass emission filter. Images (512 × 512 pixels = 520 × 520 μm, 1-bit intensity) were captured at 50–100 frames/s using a Nipkow-disk confocal scanner unit (CSU-X1; Yokogawa Electric, Tokyo, Japan), cooled CCD camera (iXON DV897; Andor, Belfast, Northern Ireland, UK), upright microscope (ECLIPSE FN1; Nikon, Tokyo, Japan) and water-immersion objective lens (16 × 0.8 NA, CFI75LWD16XW; Nikon). To extract spike activity (Sasaki *et al.*, 2008), the cell bodies of neurons were identified by visual inspection and used to place regions of interest (10-μm-radius circles) in which the fluorescence intensity was averaged across space. For each cell, the change in fluorescence ($\Delta F/F$) was calculated as $(F_t - F_0)/F_0$, where F_t is the fluorescence intensity at any time point and F_0 is the average baseline fluorescence intensity across the 10-s period before and after the focused time point. The onsets of calcium transients were semi-automatically detected using a Matlab program based on principal component analysis and support-vector machines (Sasaki *et al.*, 2008).

Detection of repeating sequences

We used a template-matching algorithm to fully search for repeating sequences (Ikegaya *et al.*, 2004). We first selected cells that exhibited more than one calcium transient. After defining the reference calcium events of the reference cell ($cell_1$), we defined a vector that consisted of a set of cells and the timing of their calcium events relative to the reference events as follows: ($cell_2$, $cell_3$, . . ., $cell_N$, t_2, t_3, . . . t_N), where t_i denotes the delay of the event of $cell_i$ relative to the reference event. t_i was limited to a time window of 500 ms or less. This vector was considered the template and was advanced forward in time through the successive events of $cell_1$ that were recorded over the remainder of the session. If more than two elements were identical between any template pairs, we regarded the matched elements as a repeating sequence. One frame jitter was allowed for detecting repeating sequences. Each mismatched spike configuration was used as another template in a subsequent scan. Thus, every event was included as part of a template sequence, and each template occurred at least once. Data are reported as the mean ± SEM.

Electrophysiological recording

Patch-clamp recordings were performed with a MultiClamp 700B amplifier and a Digidata 1440A digitizer controlled by pCLAMP 10 software (Molecular Devices, Union City, CA, USA). For whole-cell recordings, borosilicate glass pipettes (4–6 MΩ) were filled with an internal solution consisting of (in mM): K-gluconate, 135; KCl, 4; HEPES, 10; phosphocreatine-Na_2, 10; Na_2-GTP, 0.3; Mg-ATP, 4; Alexa Fluor 594 hydrazide, 200 μM (Invitrogen; pH 7.2). Excitatory and inhibitory postsynaptic currents (PSCs) were isolated by clamping at −70 mV and 0 mV, respectively. For loose cell-attached recordings, glass pipettes were filled with aCSF. Signals were low-pass filtered at 1–2 kHz, digitized at 10 kHz, and analysed with pCLAMP 10 software. In some experiments, local field potentials were recorded during fMCI monitoring of the calcium activity of CA3 neurons. Glass pipettes were filled with 2 M NaCl and placed in CA3 stratum pyramidale. To extract the ripple wave activity, the recorded data were band-pass filtered at 150–250 Hz. Ripple-like events were automatically detected based on their oscillatory powers and durations; the root mean square (3-ms window) of the band-passed signal was used to detect the ripple wave with a power threshold of 5 SDs of 10 ms in duration.

Detection of inhibitory neurons by ROTing

To identify presynaptic inhibitory neurons located within an imaging region, we utilized the ROTing technique (Sasaki *et al.*, 2009; Takahashi *et al.*, 2010). After monitoring ongoing activity with calcium imaging as described above, the extracellular solution was changed to modified aCSF, containing (in mM): K^+, 2.2; Mg^{2+}, 3.0; Ca^{2+}, 3.2; to reduce intrinsic activity and the plasticity of the synaptic wiring (Fig. 2). In addition, excitatory neurotransmission was inhibited by applying 50 μM 6-cyano-7-nitroquinoxaline-2,3-dione (CNQX) and 50 μM D,L-2-amino-5-phosphonopentanoic acid (AP5) to block the α-amino-3-hydroxy-5-methyl-4-isoxazolepropionic acid (AMPA)/kainate and *N*-methyl-D-aspartate (NMDA) receptors, respectively. After obtaining whole-cell recordings from one-three pyramidal cells with a holding voltage of 0 mV, another glass pipette (~1 MΩ) filled with 50 mM K^+ in aCSF was placed 20 μm above the surface of the slice, and high K^+ was iontophoretically applied by injecting negative rectangular 3–30 μA currents through the electrode for 1–5 s. The currents were intermittently applied at intervals of 3–5 s to avoid excessive neuronal activation due to the extracellular accumulation of K^+. This procedure evoked calcium transients in a few of the CA3 neurons located within an imaging region. The pipette was slowly moved over the CA3 networks, and the evoked calcium transients were monitored at 50 frames/s. The timings of these events were compared online with PSCs recorded

concurrently in the patch-clamped neurons, and presynaptic inhibitory neurons that were responsible for the focused PSCs were statistically screened. More specifically, for every presynaptic candidate and the frequency of background PSCs, we calculated the probability (P-value) that the observed number of coincident spikes and synaptic currents would occur if they behaved as independent Poisson units (for more detail, see Sasaki *et al.*, 2009). Neurons with a P-value < 0.01 were considered putative presynaptic cells. Using this screen, we detected presynaptic neurons with a false-positive error of $< 1\%$ and a false-negative error of 4% (Sasaki *et al.*, 2009). When a barrage of PSCs with inter-event intervals (IEIs) < 50 ms was observed in the patched neuron, only the first PSC was considered in the analysis, and the subsequent PSCs were ignored because they could have arisen from burst firing in the same presynaptic inhibitory neuron.

Prediction of repeating sequences

We examined whether the activity patterns of individual cells could serve as predictors of the emergence of repeating events. For this purpose, we used a cross-validation analysis in which each dataset was equally divided into two parts; the first part and the last part were used as a training (learning) phase and a test (event detection) phase, respectively. In the training phase, we designated an N-dimensional vector $\vec{X}_t$ (termed prediction vector) that consisted of the ratio of the number of calcium events that occurred from 0 to 100 ms before the onset of sequences to the total event number in individual cells, where N denotes the numbers of recorded neurons. Thus, the prediction vector reflects a series of the prediction probabilities that one sequence emerges 0–100 ms after the calcium events of the corresponding neurons. In the test phase, the prediction vector was used to predict the times of repeating sequences. At a time point t, we designated an N-dimensional vector $\vec{X}_t$ that consisted of the number of calcium events observed during the 100-ms period from $t-100$ (in ms) to t (in ms) in individual neurons. The product $\vec{X}' \cdot \vec{P}$ denotes the predicted probability $\vec{P}_{\mathrm{pred}}(t)$ that a sequence may start at the time point t. A predicted event was defined in the case that $\vec{P}_{\mathrm{pred}}$ exceeds 0.5. To quantify the success of the prediction, we calculated the prediction scores, which represent the ratio of the number of the predicted events that correctly coincided with the actual timings of sequence emergence to the total number of predicted events.

Results

Temporally precise sequences of neuronal events

Cortical microcircuits in slice preparations are reported to exhibit precisely timed firing patterns that can be repeated in the same sequential order (Ikegaya *et al.*, 2004; Luczak *et al.*, 2007; Matsumoto *et al.*, 2013). We first confirmed whether precise repetitions of neuronal activity were also emitted by our hippocampal slice culture preparations. We loaded neurons with OGB-1AM and monitored the ongoing activity patterns from 125 ± 6 neurons using fMCI at a frame rate of 50–100 Hz (Fig. 1A; $n = 5$ slices). In this imaging method, the action potentials of a given neuron are measured as transient calcium events in the cell body of the neuron (Fig. 1B). In our imaging condition, the average $\Delta F/F$ amplitude of calcium transients associated with single spikes was 10.4 ± 2.5%, and the signal-to-noise ratio was 11.3 ± 1.5, which allowed us to reliably detect individual single spikes. It should be noted, however, that individual spikes in bursts with a frequency of > 5 Hz were inseparable in fluorescent traces due to the temporal accumulation of calcium transients owing to their slow decay kinetics (τ = 400–600 ms; for more detail, see Sasaki *et al.*, 2008). The length of single movies was 26 000 ± 2740 frames (i.e. 460 ± 67 s). During this imaging period, the percentage of active neurons was 47 ± 7% and the frequency of neuronal events per cell was 2.0 ± 0.6 min. We used a template matching algorithm that searches for the repeated activation of 'fixed' sequences, which are defined as a subset of neurons that fire sequentially with the same order and the same delay. We referred to these precise repetitions as repeating sequences. In each dataset, a diverse repertoire of repeating sequences was detected (an example is shown in Fig. 1C and D). Single sequences appeared 2.6 ± 0.2 times (range, two-eight times; $n = 1051$ sequences from five slices), and 42.0 ± 3.9% of calcium events participated in at least one sequence ($n = 8846$ events from five slices). To evaluate the significance of sequence emergence, the number of repeating sequences in the physiological datasets was compared with those in surrogate datasets. Here, we employed two shuffling methods: (1) IEIs were randomly shuffled within each cell; and (2) single events of two randomly selected cells were repeatedly exchanged (Ikegaya *et al.*, 2004; Sasaki *et al.*, 2007). IEI shuffling eliminates the temporal correlation among cell populations but preserves the firing rates of individual neurons, whereas event pair exchange eliminates the precise orders of active cells but preserves the firing rates of individual neurons and the times of global population activity. For each original dataset, 20 surrogates were created (Fig. 1C, right). In all slices tested, significantly fewer repeating sequences were found in surrogate datasets; the real-to-surrogate ratios of the number of neurons involved in a single repeating sequence were 2.4 ± 0.2 and 2.2 ± 0.2 in IEI shuffling and event pair exchange methods, respectively, which were significantly higher than 1 (IEI shuffling, $P = 0.016$, $t_4 = 3.05$, paired t-test; event pair exchange, $P = 0.010$, $t_4 = 4.61$). This value increased as the number of neurons increased (Fig. 1E), which indicates that repeating sequences with larger numbers of neurons emerged with higher fidelity. Simultaneous recordings of extracellular signals and population events demonstrated that repeating sequences were associated with ripple oscillations that were detected by filtering CA3 local field potentials at 150–250 Hz (Fig. 1F and G). Overall, 32% of repeating sequences were correlated with the timing of ripple oscillations. The mean duration of the sequences was 163 ± 83 ms; this time scale is in accordance with *in vivo* observations that behavioral sequences in hippocampal place cells are replayed within a time window of hundreds of milliseconds during SW-Rs (Foster & Wilson, 2006; Diba & Buzsaki, 2007; Karlsson & Frank, 2009; Dragoi & Tonegawa, 2011).

Identifying inhibitory neurons by ROTing

Having statistically confirmed the occurrence of repeating sequences, we next examined how the repeating sequences are coordinated by excitatory and inhibitory neuronal populations. To identify inhibitory interneurons in an imaging region, we applied the ROTing technique, a modified method from reverse optical probing (Aaron & Yuste, 2006), which searches for presynaptic neurons by simultaneously monitoring the firing activity of individual neurons and PSCs from patch-clamped neurons (Sasaki *et al.*, 2009). The concept of ROTing is illustrated in Fig. 2A–E; if neuron A repeatedly displays calcium events that are time-locked to the timing of inhibitory PSCs recorded from neuron B, neuron A is a putative presynaptic interneuron that sends inhibitory inputs to neuron B. We have previously shown that this method can detect presynaptic neurons